Adsorption of Rhodamine B from Aqueous Solution Using Treated Epicarp of Raphia Hookerie

By

A.A. Inyinbor[*a,b] ,

F.A. Adekola,[b]

&

G.A. Olatunji[b]

[a]Department of Physical Sciences,
Landmark University, P.M.B 1001, Omu Aran, Nigeria.
[b]Department of Chemistry,
University of Ilorin, P.M.B 1515, Ilorin, Nigeria.

Corresponding Authors E-mail:
inyinbor.adejumoke@landmarkuniversity.edu.ng

Abstract: Modified *Raphia hookerie* waste (CMRH) was prepared and utilized for the uptake of rhodamine B (RhB). The adsorbent was characterized using Fourier transform infra red (FTIR), Brunauer– Emmett–Teller (BET) and Scanning Electron Microscopy (SEM). FTIR analysis revealed functional groups such as C-N, C-OH and S-H which are good adsorption site for cationic toxicants. The surface area of the modified *Raphia hookerie* was observed to be low (6.25 m^2/g), however modification was observed to increase the surface area of adsorbent when compared with that of raw *Raphia hookerie* (0.04 m^2/g). The sorption data fitted better into the Freundlich adsorption isotherm than the Langmuir, the maximum sorption capacity q_o as obtained from the Langmuir adsorption parameters was 357.14 mg/g. Sorption energy obtained for Dubinin–Radushkevich (D-R) isotherm for the adsorption process was found to be less than 8 KJ mol^{-1} which suggest that uptake of RhB onto CMRH was physical in nature.

Key words: *Raphia hookerie*, Modification, Adsorption, Rhodamine B, BET, SEM, FTIR.

1.0 Introduction

Textile industries use large volume of water in their various operations and manufacturing stages hence discharge large volumes of waste water into the environment. Waste water generated from dye preparation, spent dye bath and washing processes usually contribute a larger percentage of the textile industries waste water. Dye poses various threats to the environment

and also the most difficult constituent of the textile waste water to treat [1]. Various types of dyes such as acidic, basic, reactive, azo, diazo, anthraquinone base-metal complex are in use in textile industries and these dyes are usually characterized by high molecular weight and complex chemical structures hence showing low level of biodegradability [2,3].

Various conventional methods exist for the treatment of industrial waste water, which are characterized by economical disadvantages and/or ineffectiveness in the removal of very low concentration of pollutants. Adsorption unto activated carbon is characterized by simple operation and design. Activated carbon has the ability to adsorb broad range of pollutants and its fast adsorption kinetics makes it superior to other conventional methods [4].

Low cost adsorbent have been utilized as alternative adsorbent to activated carbon which is prepared from expensive precursors thus making them very expensive. Low cost adsorbent which is captured within the 'green chemistry' enhances environmental sustainability and can remove very low concentration of toxicants at a very low cost. However surface modification or functionalization could greatly improve the sorption capacity of biomaterials [5].

Raphia hookerie is a member of the *aracacea* or *Palmacea* family. Other members of this family such as the cocos nucifera have been utilized as low cost adsorbent and as precursors for activated carbon preparations and they have been found to be very effective [4,6,7,8]. However, to the best of our knowledge no report is available for the use of *Raphia hookerie* as either low cost adsorbent or precursor for activated carbon preparation. Therefore the aim of this work is to prepare a modified low cost adsorbent from the epicarp of *Raphia hookerie* (cysteine modified *Raphia hookerie* : CMRH), characterize the prepared adsorbent and to apply same in the uptake of a cationic dye (rhodamine B: RhB).

2.0 Materials and methods

All reagents were of analytical grade, cysteine was supplied by Sigma Aldrich and Rhodamine B was supplied by BDH. Characteristics of RhB is as shown in Table 1 and structure of RhB in Figure 1.

Table 1: Properties of rhodamine B.

Parameters	Values
Suggested name	Rhodamine B
C.I number	45170
C.I name	Basic violet 10
Class	Rhodamine
λ_{max}	554nm

Molecular formula	$C_{28}H_{31}N_2O_3Cl$
Formula weight	479.02

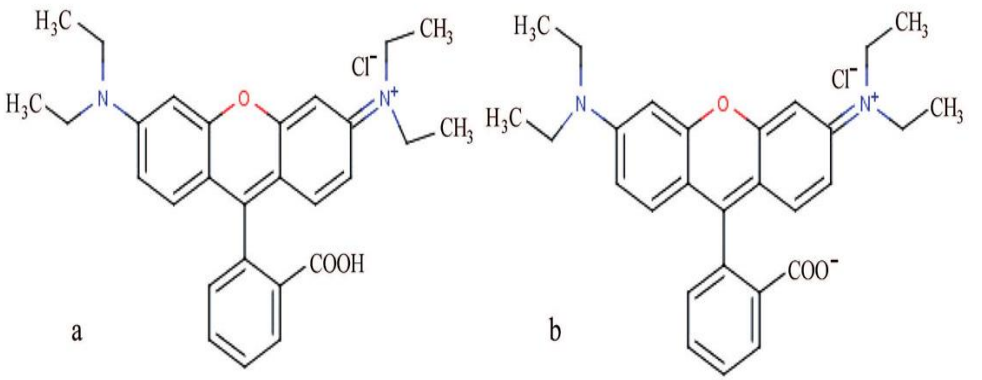

Figure 1: Structure of Rhodamine B (a) Cationic (b) Zwitterionic

2.1 Preparation of sorbent

2.1.1 Cysteine modified Raphia hookerie

Epicarps of Raphia hookerie were collected from local farmers in Mokogi, Edu local government area of Kwara state, Nigeria. It was thoroughly washed to remove dirts and dried in an oven overnight at 105^{o}C. It was then pulverized and screened into a particle size of 150-250µm. Cysteine modification was done according to the methods described by Faghihian and Nejati-Yazdinejad, [9], 10 g of biomass was suspended in 100 cm^3 cysteine solution (pH 4.8), the mixture was agitated for 12 hours, filtered, washed to neutrality and dried at room temperature. The dried Cysteine modified biomaterials were stored in air tight containers.

2.1.2 Characterization of CMRH

CMRH was characterized using scanning electron microscope (SEM), energy dispersive X-ray (EDX) and Fourier transform infrared (FTIR) and Brunauer–Emmett–Teller (BET).

2.1.3 Batch adsorption studies

Batch adsorption studies with respect to initial pH, initial dye concentration, adsorbent dosage and temperature were carried out. Adsorption processes were performed by agitating a given dose of the adsorbent with 100 cm^3 of RhB solution of desired concentration in different 250 cm^3 flasks in a temperature controlled water bath shaker. A shaking speed of 130 rpm was maintained throughout the experiment to achieve equilibrium. Desired pH was obtained by adding HCl and NaOH

(0.1M). Samples were withdrawn at different time intervals, centrifuged and the supernatant was analyzed for change in dye concentration using a UV–Visible spectrophotometer. The λ_{max} of RhB was earlier obtained to be 554nm by scanning using different concentrations of RhB solution in a Beckman Coulter Du 730 UV/Vis spectrophotometer. All readings were taken in triplicates and the mean considered in data analysis. The quantity of dye adsorbed at a given time q_t (mg/g) and percentage dye removed were calculated according to the mathematical expressions below;

$$q_t = \frac{(C_i - C_t)}{M} \times V \quad (1)$$

$$\% \text{ Removal} = \frac{(C_i - C_t)}{C_i} \times 100 \quad (2)$$

Where C_i and C_t are concentrations of RhB in solution at initial and at time t, V is the volume in liter and M is the weight of the adsorbent in g.

2.5 Desorption experiment

In order to investigate the leaching/desorption of RhB from CMRH, deionized water, 0.1M HCl and 0.1M CH_3COOH were used as desorbing agents. 0.1 g of fresh adsorbent was added to 100 cm^3 of 100 mgL^{-1} RhB solution at pH 3.0 and shaken for 50 minutes. The RhB-loaded sorbents were separated by centrifugation and the residual RhB concentration were determined using spectrophotometer as earlier described. The RhB loaded sorbents were washed gently with water to remove any unadsorbed dye and dried. The desorption process was carried out by mixing 100 cm^3 of each desorbing agents with the dried sorbents and shaken for a predetermined time and the desorbed RhB was determined spectrophotometrically. The desorbing efficiency was then calculated using the mathematical relation below;

$$\text{Desorption efficiency (\%)} = \frac{q_{de}}{q_{ad}} \times 100 \quad (3)$$

Where q_{de} is the quantity desorbed by each eluent and q_{ad} is the quantity of RhB adsorbed during the loading.

3.0 Results and Discussions

3.1 Characteristics of the prepared Adsorbents

3.1.1 Physicochemical parameters and Surface Morphology

Table 2: Characteristics of CMRH

Parameters	Values
	CMRH
pH	5.72
PZC	6.00
Bulk density	0.24
Moisture content (%)	3.33
Ash content (%)	3.70
BET surface area (m^2/g)	6.25
Average pore diameter(nm)	784.20

Table 2 depicts the characteristics of CMRH, the surface areas of the sorbent is observed to be low, low surface area is the characteristics of

agro waste and this has been previously reported by others [10,11]. Figure 2 (a and b) shows the topography of CMRH before and after dye adsorption, CMRH was observed to have tiny perforations and deep hollows like crevices of a mountain (Figure 2a). However after dye adsorption the adsorbate covered the surface of the pores earlier observed (Figure 2b). EDX spectrum (Figure 3) shows that CMRH contain 69.04% carbon, 29.79% oxygen and 0.73% of calcium, the presence of Ca^{2+} present a possibility of ion exchange with cationic species.

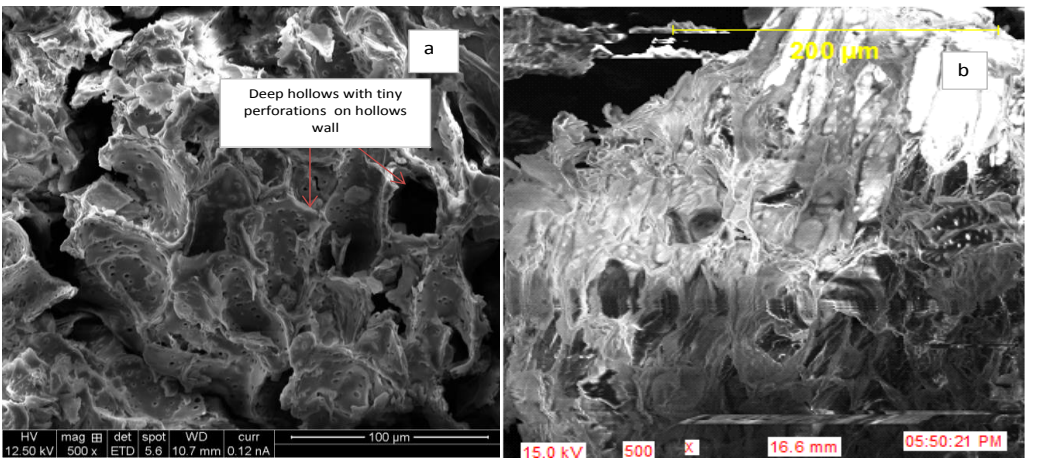

Figure 2: SEM micrograph of CMRH (a) before dye sorption (b) after dye sorption

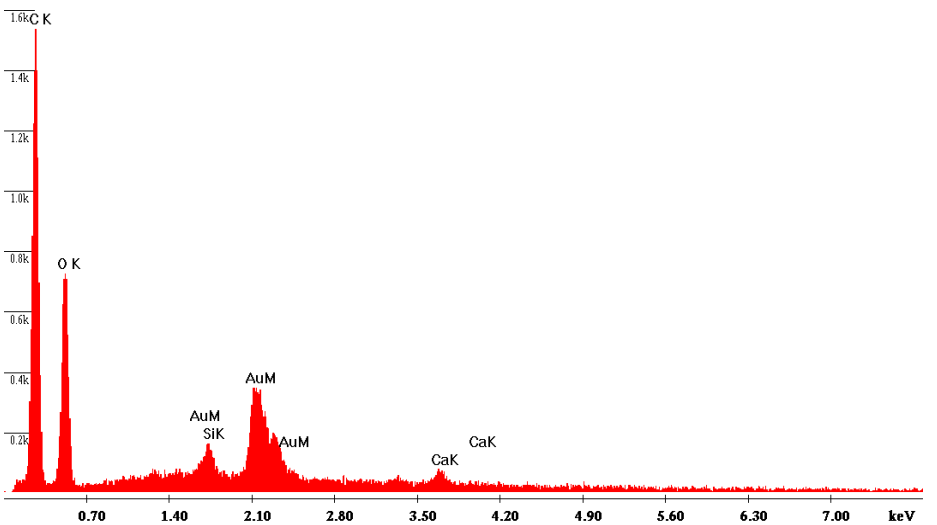

Figure 3: EDX spectrum of CMRH

3.1.2 FTIR analysis

Intense bands were observed at 1237.90 cm^{-1}, 3279.45 cm^{-1} and 1033.41 cm^{-1}which corresponds to C-N stretching, O-H of alcohol and C-OH stretching vibrations respectively (Figure 4a). Other bands were observed at 2911.79 cm^{-1} and 2580.87 cm^{-1} which corresponds to C-H stretching and S-H from cysteine. After adsorption, there was a shift of C-N, C-H, C-OH and –OH bands to 1246.06 cm^{-1}, 2935.76 cm^{-1}, 1047.38 cm^{-1} and 3421.83 cm^{-1} respectively (Figure 4b). This suggests that these functional groups participated in the adsorption of RhB [12]. New peaks were also observed at 1593.25 and 1735.99 cm^{-1} (Figure 4b) which corresponds to carboxylate ion and aromatic rings from RhB.

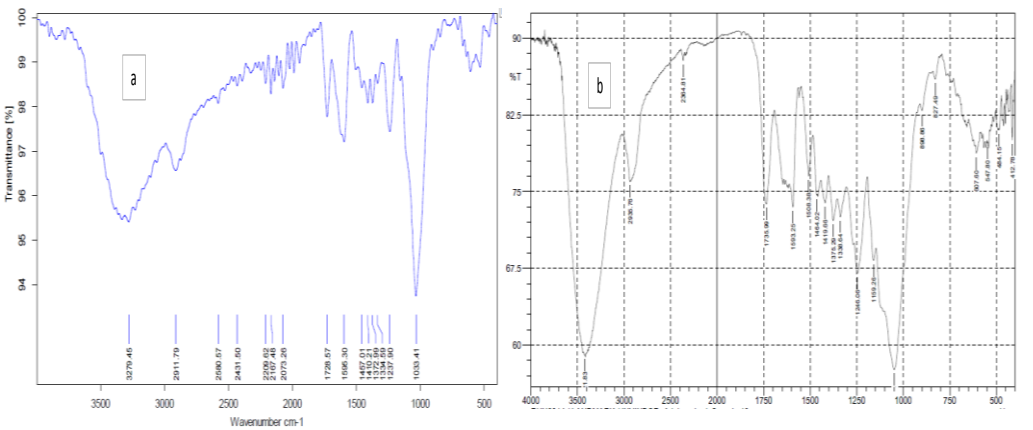

Figure 4: FTIR spectra of CMRH (a) Before dye adsorption and (b) After dye adsorption

3.2 Effects of pH

Percentage adsorption was observed to increase gradually from pH 2 to 3 and decreased gradually as the pH increased (Figure 5). Optimum pH was observed at pH 3, maximum adsorption was recorded to be 74.55%. The pKa of RhB is 3.7 and above this pH deprotonation of the carboxyl functional group occurs (Figure 1a). Attraction between the carboxylate ion (Figure 1b) and the xanthene groups results in the formation of dimers of RhB thereby resulting in decreased adsorption. Optimum adsorption of RhB between pH 3 and 4 has previously been reported by research [13,14].

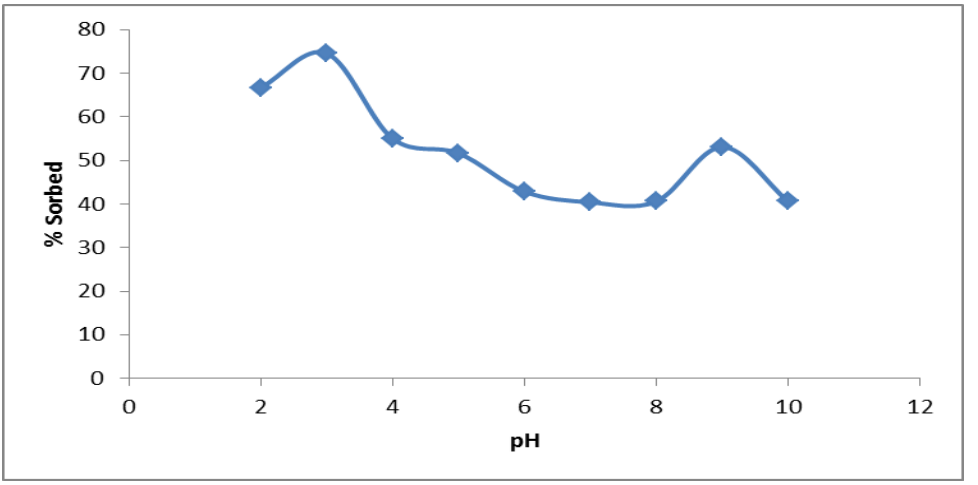

Figure 5:Effect of pH on the percentage removal of Rhodamine B by CMRH [Adsorbent dose (1gL^{-1}), agitation speed (130 rpm), agitation time (120 minutes), Temperature (26±2^{o}C), Adsorbate concentration (100 mgL^{-1})].

3.3 Effect of concentration and contact time

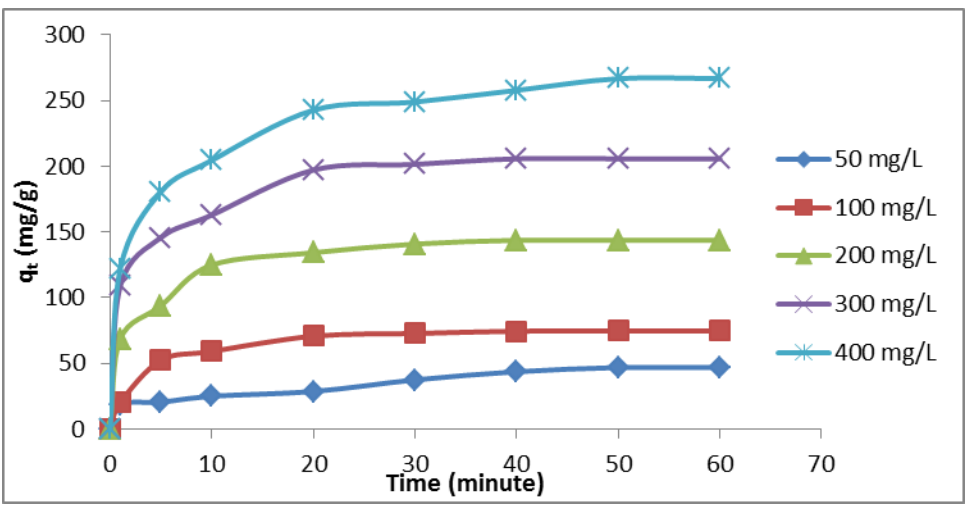

Figure 6: Effects of contact time and initial dye concentration on the uptake of RhB unto CMRH
[Adsorbent dose (1 gL^{-1}), agitation speed (130 rpm), Temperature (26±2^{o}C), pH (3)].

Figures 6 depicts the sorbate-sorbents interactions as a function of time and concentration (50-400 mgL^{-1}). The uptake of RhB onto CMRH (figure 6) was observed to be rapid initially and gradually tends to

equilibrium. Quantity sorbed at a given time t (q_t) increased with increase in initial dye concentration, equilibrium was attained at 40 minutes for initial RhB concentration of 100, 200 and 300 mgL^{-1} and at 50 minutes for 50 mgL^{-1} and 400 mgL^{-1}. The amount sorbed at equilibrium increased from 46.88 mgg^{-1} for initial dye concentration of 50 mgL^{-1} to 266.67 mgg^{-1} for initial dye concentration of 400 mgL^{-1}.

3.4 Effects of Adsorbent Dosage

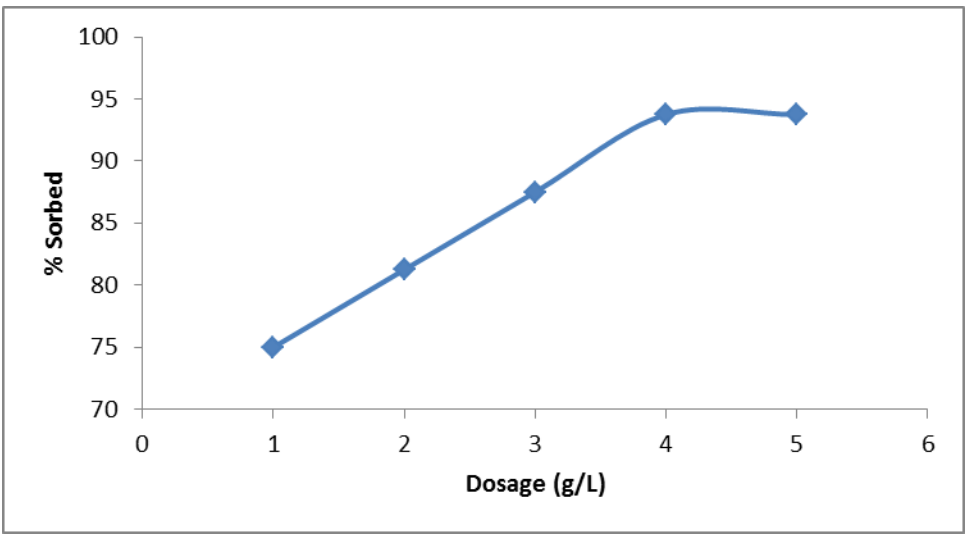

Figure 7: Effects of sorbent dosage on the uptake of RhB unto CMRH [Initial concentration (100 mgL^{-1}), agitation speed (130 rpm), Temperature (26±2^{o}C), pH (3)].

Figure 7 depicts the percentage adsorbed as related to adsorbent dosage. Percentage adsorbed increased from 75% to 93.75% from 1 to 3 and to 4 gL^{-1} adsorbent dose, however there was equilibrium between 4 gL^{-1} and 5 gL^{-1}. increase in available surface area resulted into increase in percentage adsorption.

3.5 Effects of Temperature and Thermodynamic Studies

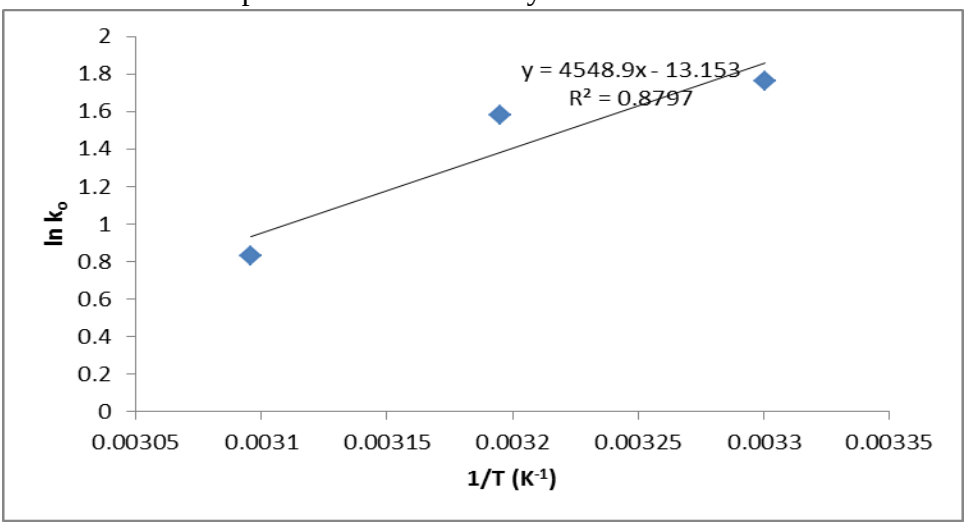

Figure 8: Effects of Temperature on the uptake of RhB unto CMRH [Initial concentration (100 mgL^{-1}), agitation speed (130 rpm), Adsorbent dosage ($1gL^{-1}$), pH (3)].

Figure 8 shows the effect of temperature on the adsorption of RhB onto CMRH, the uptake of RhB was observed to decrease from about 85% to about 69% as the temperature increased from 303 to 323 K. Thermodynamic parameters ΔG^o, ΔH^o and ΔS^o, which are important in determining the feasibility, spontaneity and the nature of adsorbate-adsorbent interactions, were calculated. The thermodynamic parameters were obtained using the mathematical relation below;

$$\ln K_o = \frac{\Delta S^o}{R} - \frac{\Delta H^o}{RT} \quad (4)$$

$$\Delta G^o = -RT\ln K_o \quad (5)$$

Where K_o is given as q_e/C_e, T is the temperature in Kelvin and R is the gas constant. A plot of $\ln K_o$ versus 1/T gave a linear plot (Figure 8) and ΔH^o and ΔS^o were calculated from the slope and intercept respectively. Negative enthalpy (ΔH^o= -37.82 KJ mol^{-1}) obtained indicates that the adsorption process is exothermic in nature. The negative values of ΔS^o (-109.35 $Jmol^{-1}K^{-1}$) indicate decrease in the randomness at the solid-liquid interface during sorption of RhB onto CMRH and the high negative value of ΔS^o suggests stability of RhB on the surface of CMRH. The values of ΔG^o obtained were -4.443, -4.108 and -2.222 KJ mol^{-1} for 303, 313 and 323 K respectively. The negative values of ΔG^o suggest that the sorption process was spontaneous; more negative values at lower temperature suggest that sorption process at lower temperature was more spontaneous. Similar trends have been reported by other researchers [11,15].

3.6 Adsorption Kinetics

Sorption data were tested using the pseudo-first-order, pseudo-second-order and the intra particle diffusion models in order to establish the best kinetic model and mechanism that best describe the adsorption process.

3.6.1 Pseudo-first-order kinetic

The pseudo first-order kinetic model of Lagergren given by the mathematical expression below [16];

$$\ln(q_e-q_t) = \ln q_e - k_1 t \qquad (6)$$

Where q_e and q_t are quantities absorbed at equilibrium and at time t respectively (mgg^{-1}), and k_1 is the rate constant for the pseudo-first-order sorption (min^{-1}). A plot of $\ln(q_e-q_t)$ against t for various concentrations of RhB resulted in linear graphs with negative slopes (Figure 9). k_i and the calculated quantity adsorbed (q_{cal}) were determined from the slope and intercept respectively (Table 3). The q_{cal} values for each concentration were observed to vary considerably from the experimentally determined quantity adsorbed (q_{exp}) values. This suggests that the data does not fit well into this kinetic model.

3.6.2 Pseudo-second-order kinetic

The pseudo-second-order kinetic model given by the mathematical expression below [17];

$$dq_t/dt = k_2(q_e-q_t)^2 \qquad (7)$$

Where K_2 is the rate constant of the pseudo-second-order equation in g mg^{-1} min^{-1}, q_e is the maximum sorption capacity in mg g^{-1} and q_t (mg g^{-1}) is the amount of sorption at time t.

Integration and rearrangement of equation (7) above will give a linear form

$$t/q_t = 1/k_2q_e^2 + 1(t)/q_e \qquad (8)$$

A plot t/q_t against t gave linear graphs (Figures 10) and the values of q_e and k_2 were calculated from the slope and intercepts of the graphs. The R^2 values obtained were higher than those obtained for the pseudo-first-order kinetics and there was a good agreement between the q_e calculated and the q_e experimental (Table 3). This shows that the pseudo-second-order kinetic fits the sorption data better.

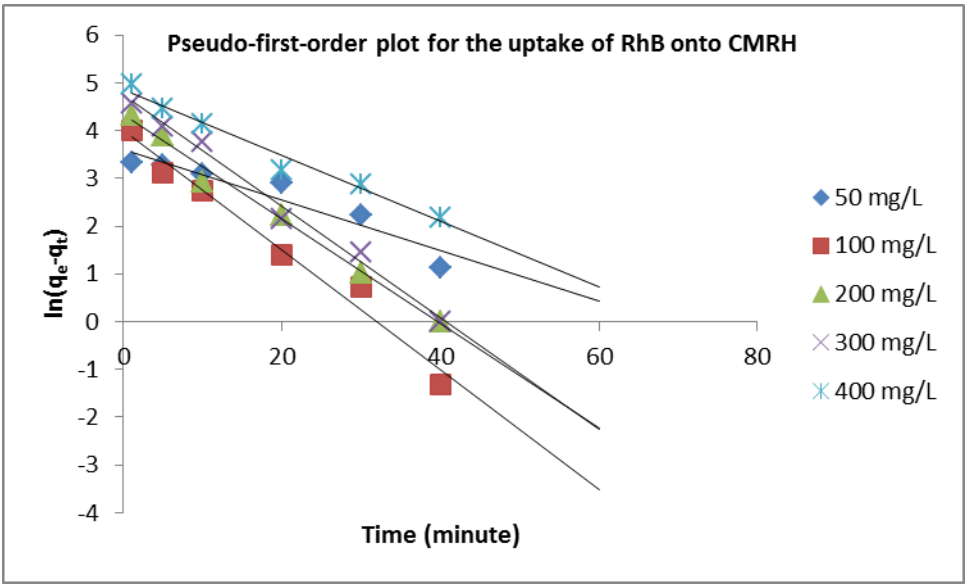

Figure 9: Pseudo-first-order plot for the uptake of RhB onto CMRH [Initial concentration (50-400 mgL^{-1}), agitation speed (130 rpm), Adsorbent dosage ($1gL^{-1}$), pH (3)].

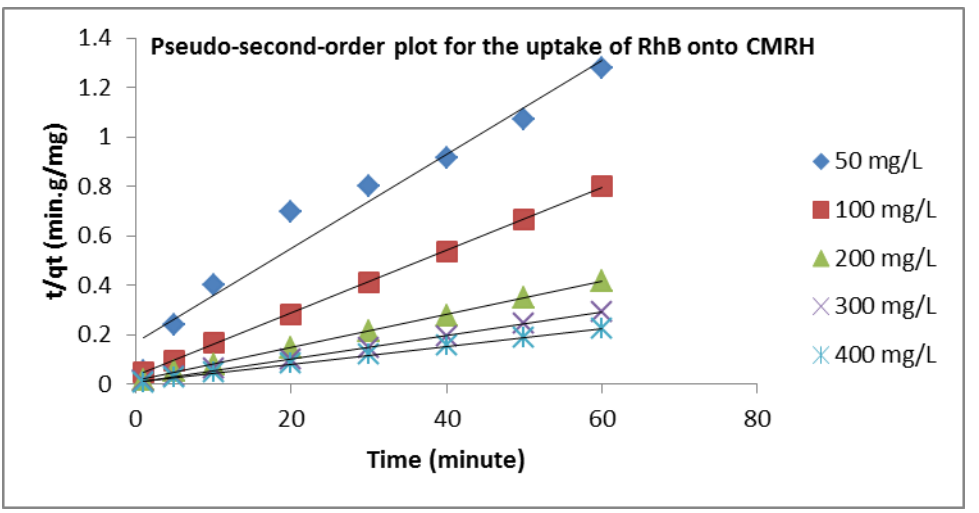

Figure 10: Pseudo-second-order plot for the uptake of RhB onto CMRH [Initial concentration (50-400 mgL^{-1}), agitation speed (130 rpm), Adsorbent dosage ($1gL^{-1}$), pH (3)].

3.6.3 Intra-particle diffusion model
The intra-particle diffusion model given by the mathematical expression below [18];

$$qt = K_{diff}\, t^{1/2} + C \qquad (9)$$

Where q_t (mgg^{-1}) is the amount of RhB dye absorbed at time t and K_{diff} ($mgg^{-1}min^{-1/2}$) is the rate constant for intra-particle diffusion. The value of C explains the thickness of the boundary layer, the larger the intercept the greater the boundary layer effect. A plot of q_t versus $t^{0.5}$ gave a linear graph (Figure 11) and the values of the R^2 ranges 0.7643 to 0.9621 (Table 3) suggesting that the sorption of RhB unto CMRH may be controlled by intra-particle diffusion model.

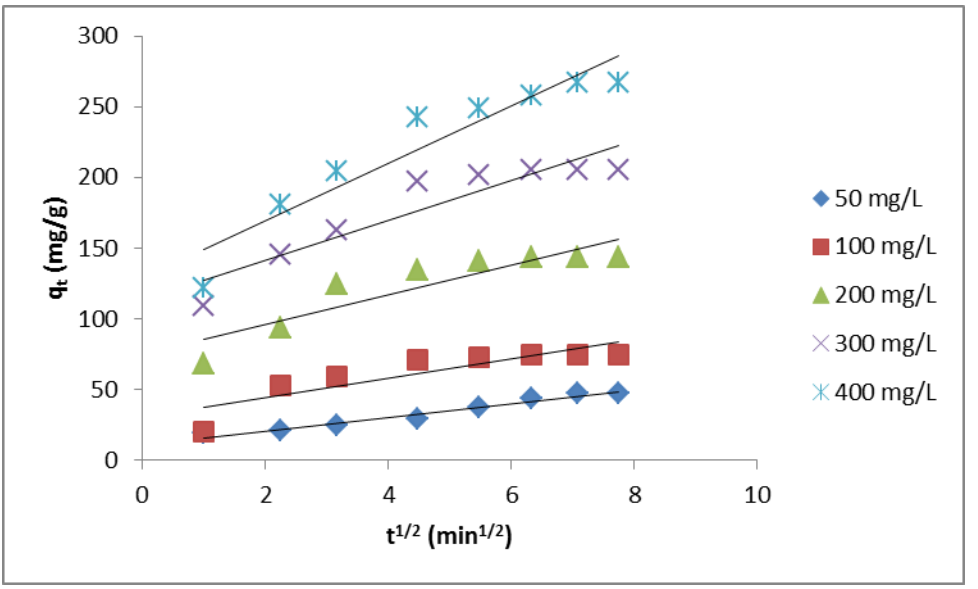

Figure 11: Intra-particle diffusion model for the uptake of RhB onto CMRH [Initial concentration (50-400 mgL^{-1}), agitation speed (130 rpm), Adsorbent dosage ($1gL^{-1}$), pH (3)].

Table 3: Comparison of Pseudo-first-order, Pseudo-second-order and intra particle diffusion kinetic model

Constants	Initial concentration				
	CMRH				
	50	100	200	300	400
$q_{e\ experimental}$ (mgL^{-1})	46.88	74.83	143.66	205.70	266.67
Pseudo-first-order					
$q_{e\ calculated}$ (mgL^{-1})	36.33	54.05	76.35	112.49	127.68
$K_1 \times 10^{-2}$ (min^{-1})	5.27	12.52	10.92	11.61	6.88

R^2	0.90	0.98	0.99	0.99	0.97
Pseudo-second-order					
$q_{e\ calculated}$ (mgL^{-1})	52.36	78.74	149.25	212.77	277.77
$K_2 \times 10^{-3}$($gmg^{-1}min^{-1}$)	2.20	4.74	3.40	2.50	1.35
R^2	0.96	0.99	0.99	0.99	0.99
Intra particle diffusion					
$C \times 10^2$ (mgg^{-1})	0.11	0.29	0.75	1.13	1.29
K_{diff}($mgg^{-1}min^{-1/2}$)	4.78	6.92	10.59	14.08	20.26
R^2	0.96	0.76	0.82	0.86	0.89

3.7 Adsorption Isotherms

Adsorption isotherm can be described as an invaluable curve that describes the phenomenon governing the retention (or release) or mobility of a substance from the aqueous porous media or aquatic environments to a solid-phase at a constant temperature and pH. The adsorption data were tested using the Langmuir, Freundlich and Dubinin–Radushkevich (D–R) isotherm models.

3.7.1 Langmuir isotherm model

The linearized Langmuir adsorption model expressed by the mathematical expression below [19],

$$\frac{C_e}{q_e} = \frac{C_e}{q_o} + \frac{1}{q_o K_L}$$

Where C_e is the concentration of RhB dye in the solution at equilibrium ($m \cdot L^{-1}$), q_e is the concentration of RhB dye on the adsorbent at equilibrium ($mg \cdot g^{-1}$), q_o is the monolayer adsorption capacity of adsorbent ($mg \cdot g^{-1}$) and K_L is the Langmuir adsorption constant ($L \cdot mg^{-1}$). A straight line graph is expected for the plot of C_e/q_e versus C_e with slope $1/q_o$ and an intercept of $1/q_o K_L$. Figure 12 depicts plot of C_e/q_e versus C_e for the uptake of RhB unto CMRH. Values of q_o and K_L are calculated and reported in Table 4. The favorability of the adsorption process was also confirmed by calculating the dimensionless equilibrium parameter (R_L) expressed by Equation (11) below;

$$R_L = \frac{1}{1+K_L C_o} \qquad (11)$$

Where C_o is the highest initial dye concentration in solution. The adsorption process is said to be favorable if

R_L value falls between 0 and 1 i.e ($0 < R_L < 1$), linear when $R_L = 1$, irreversible when $R_L = 0$ and unfavorable when $RL > 1$ [19]. The value of R_L obtained is reported in Table 4 (R_L =0.134), this suggests the favorability of the adsorption process. The maximum monolayer adsorption capacity (q_{max}) was obtained to be 357.14 mgg^{-1}.

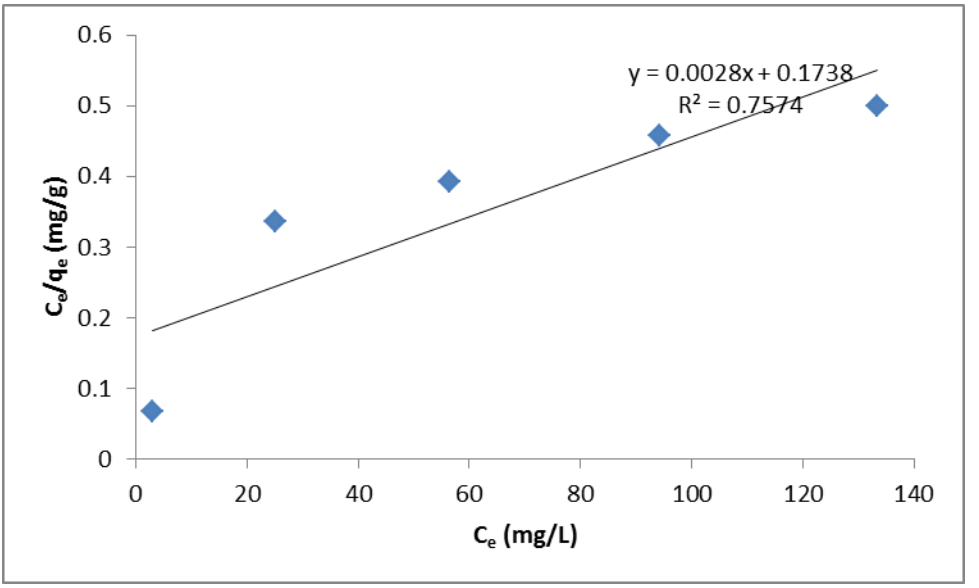

Figure 12: Langmuir isotherm plots for adsorption of RhB unto CMRH at different initial dye concentrations. [pH = 3, dose = 1 gL^{-1} and temperature (26±2^{o}C)]

3.7.2 Freundlich Isotherm Model

The linearized form of Freundlich model is expressed according to the mathematical expression below [20];

$$\log q_e = \frac{1}{n} \log C_e + \log K_f \qquad (12)$$

Where qe is the amount of RhB dye adsorbed at equilibrium ($mg \cdot g^{-1}$), C_e is the equilibrium concentration of the adsorbate ($mg \cdot L^{-1}$); K_f and n are constants incorporating the factors affecting the adsorption capacity and the degree of non-linearity between the solute concentration in the solution and the amount adsorbed at equilibrium respectively. The Plots of log q_e against log C_e gave a linear graph (Figure 13) with R^2 of 0.916. Comparing the R^2 values of Langmuir and Freundlich isotherms, the adsorption data fits the Freundlich model better (Table 4). The values of K_f and n obtained from the slopes and intercepts of the graph are also reported in Table 4. The values of n were observed to be greater than 1 which suggests that the sorption process is favorable.

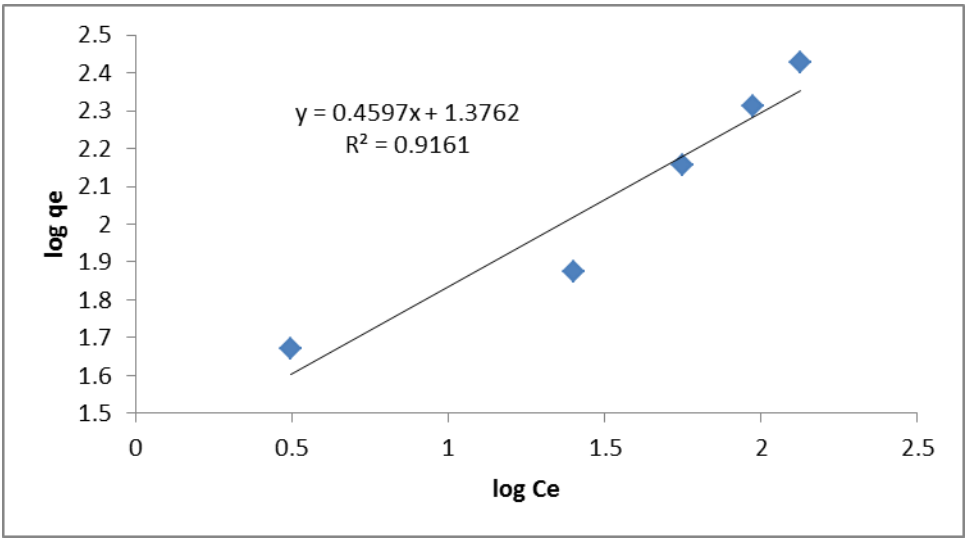

Figure 13: Freundlich isotherm plots for adsorption of RhB unto CMRH at different initial dye concentrations. [pH = 3, dose = 1 g/L and temperature (26±2^{o}C)]

3.7.3 Dubinin–Radushkevich (D–R) isotherm model

D–R model is a more general model that does not assume a homogenous surface or constant adsorption potential, D-R model gives information about sorption mechanism, whether chemisorption or physisorption [21] and it is given by the mathematical expression below;

$$\ln q_e = \ln q_o - \beta\varepsilon \qquad (13)$$

Where q_e is the amount of RhB ions adsorbed per unit weight of adsorbent (mgg^{-1}), q_o is the maximum sorption capacity, β is the activity coefficient related to mean sorption energy E ($KJmol^{-1}$) (equation 15) and Ɛ is the Polanyi potential. Ɛ is expressed by equation 14;

$$\varepsilon = RT\ln\left(1 + \frac{1}{Ce}\right) \qquad (14)$$

$$E = \sqrt{1/2\beta} \qquad (15)$$

Where R is the gas constant ($Jmol^{-1}K^{-1}$) and T is the temperature (K). β (mol^2Jol^{-2}) and q_o can be obtained from the slope and the intercept of the plot of ln q_e vs ε^2 respectively. The plot of ln q_e vs ε^2 is presented in figure 14 and the calculated parameters listed in table 4. The calculated E value was obtained to be 1.943 $KJmol^{-1}$suggesting that the uptake of RhB by CMRH is physical in nature [22].

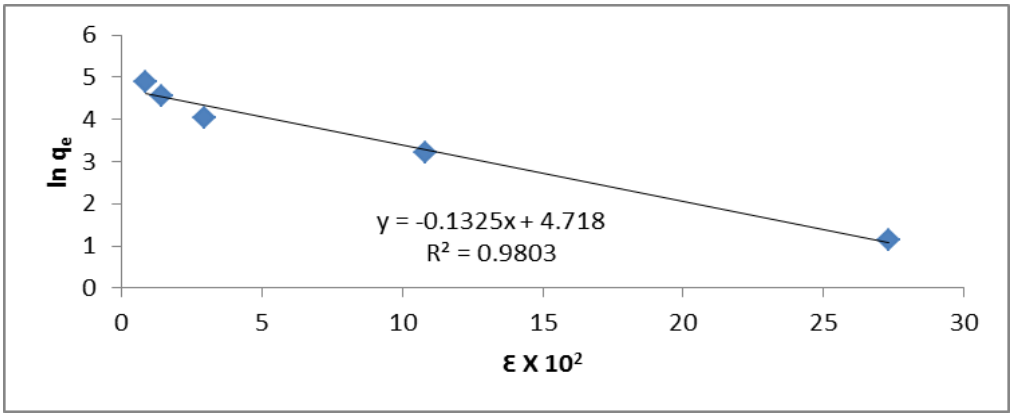

Figure 14: *Dubinin–Radushkevich (D–R)* isotherm plots for adsorption of RhB unto CMRH at different initial dye concentrations. [pH = 3, dose = 1 gL^{-1} and temperature (26±2^oC)]

Table 4: Parameters of Langmuir, Freundlich and D-R adsorption isotherm for the uptake of RhB on to CMRH.

Isotherms	constants	CMRH
Lagmuir	q_{max} (mgg^{-1})	357.14
	K_L ($L.mg^{-1}$)	0.02
	R_L	0.13
	R^2	0.76
Freundlich	K_f	23.78
	n	2.18
	R^2	0.92
DRK	q_o (mgg^{-1})	111.94
	β ($mol^2.KJ^{-2}$)	0.13
	E ($KJmol^{-1}$)	1.94
	R^2	0.98

3.8 Desorption of RhB from CMRH

Desorption studies gives an insight into the mechanisms of Biosorption and the possibility of regeneration of the adsorbent. In the case of CMRH-RhB system, the desorption efficiency for all the eluent used was not more than 25%, with water having the highest desorption efficiency (25%) followed by HCl (21.67%) and then acetic acid (8.33%). Since highest desorption efficiency was achieved using neutral pH water, this suggest that most of the dye molecule adsorbed

by CMRH had a weak attachment to the surface of the adsorbent [12].

3.9 Conclusion

Optimum adsorption was obtained at pH 3, increase in temperature from 303K to 323K decreases adsorption capacity of CMRH from about 85% to about 69%.

Pseudo-second-order kinetics better describe the adsorption process while the adsorption data fitted better into the Freundlich adsorption isotherm. The q_{max} calculated from Langmuir adsorption isotherm was 357.14 mgg^{-1}.

The value of E obtained for the D-R model suggests that the adsorption was physical in nature and since water had the highest desorption efficiency, attachment of dye to the surface of CMRH can be said to be weak.

Reference

de Menezes, E.W., Lima, E.C. Royer, B. de Souza, F.E., dos Santos, B.D. Gregório, J.R., Costa, T.M.H., Gushikem, Y. and Benvenutti, E.V. (2012) Ionic silica based hybrid material containing the pyridinium group used as an adsorbent for textile dye; Journal of Colloid and Interface Science 378:10–20.

Sathiya, M.P., Periyar, S.S., Sasikalaveni,A., Murugesan, K., and Kalaichelvan,P.T. (2007)., Decolorization of textile dyes and their effluents using white rot fungi. *African Journal of Biotechnology* **6**(4):424-429.

Yemendzhiev, H., Alexieva, Z. and Krastanov, A. (2009)., Decolorization of synthetic dye reactive blue 4 by mycelial culture of white-rot fungi *trametes versicolor* 1. *Biotechnol. & Biotechnol.* EQ **23**(3):1337-1339.

Tan, I.A.W., Ahmad, A.L. and Hameed, B.H. (2008) Preparation of activated carbon from coconut husk: Optimization study on removal of 2,4,6-trichlorophenol using response surface methodology; Journal of Hazardous Materials 153:709–717.

Puspa, L. H., Deepak, B., Hari, P. and Kedar N. G. (2009), Studies on Functionalization of Apple Waste for Heavy Metal Treatment., *Nepal Journal of Science and Technology*,(10):135-139.

Vivekanand, G. and Shankar, P.A. (2008) Surface Modification of Activated Carbon for the Removal of Water Impurities *Water Conditioning & Purification*. Available on http://www.wcponline.com/pdf/0806Gaur_Shankar.pdf

Hameed, B.H., Mahmoud, D.K. and Ahmad, A.L. (2008) Equilibrium modeling and kinetic studies on the adsorption of basic dye by a low-cost adsorbent: Coconut (*Cocos nucifera*) bunch waste; Journal

of Hazardous Materials 158:65–72.

Bello, O.S. and Ahmad, M.A. (2012): Coconut (Cocos nucifera) Shell Based Activated Carbon for the Removal of Malachite Green Dye from Aqueous Solutions, Separation Science and Technology, 47:6, 903-912.

Faghihian, H. and Massoud N. (2009) .Sorption performance of cysteine-modified bentonite in heavy metals uptake. *J. Serb. Chem. Soc.*, **74** (7): 833–843.

Martins O. O., Jonathan O. B., Emmanuel, I. U., Weiguo, S., Jian, R.G., Efficient chromium abstraction from aqueous solution using a low-cost biosorbent: Nauclea diderrichii seed biomass waste. Journal of Saudi Chemical Society (2012), http://dx.doi.org/10.1016/j.jscs.2012.09.017**.**

Zhang, Z., Ian, M.O., Geoff, K.A. and William, O.S.D. (2013) Comparative study on adsorption of two cationic dyes by milled sugarcane bagasse; Industrial Crops and Products 42:41– 49.

Bello, O.S., Ahmad, M.A. & Ahmad, N. (2012) Adsorptive features of banana (*Musa paradisiaca*) stalk-based activated carbon for malachite green dye removal. *Chemistry and Ecology*, 28 (2): 153–167.

Zamouche, M. and Hamdaoui, O. (2012) Sorption of Rhodamine B by cedar cone: effect of pH and ionic strength, Energy Procedia 18:1228 – 1239.

Gan, P.P. and Li, S.F.Y. (2013) Efficient removal of Rhodamine B using a rice hull-based silica supported iron catalyst by Fenton-like process, Chemical Engineering Journal 229:351–363.

Gupta, N., Kushwaha, A.K., and Chattopadhyaya, M.C. (2012) Adsorption studies of cationic dyes onto Ashoka (Saraca asoca) leaf powder; Journal of the Taiwan Institute of Chemical Engineers 43:604–613.

Lagergren, S. and Svenska, B.K. (1898) *On the theory of so-called adsorption of materials*, R. Swed. Acad. Sci. Doc, Band, 24:1– 13.

Ho, Y.S. and McKay, G. (1999) *Pseudo-second order model for sorption processes*, Proc. Biochem. 34:451– 465.

Weber, W.J. and Morris, J.C. (1963) *Kinetics of adsorption on carbon from solution*, J. Sanity Eng. Div. Am. Soc. Civil Eng. 89:31–59.

Langmuir, I., *The constitutional and fundamental properties of solids and liquids*, J. Am. Chem. Soc. 38 (1916), pp. 2221–2295.

Freundlich, H.M.F. (1906) *Over the adsorption in solution*, Z. Phys. Chem. 57:385–470.

Dubinin, M.M. and Radushkevich, L.V. (1947) *Equation of the characteristic curve of activated*

charcoal, Proc. Acad. Sci. Phys. Chem. USSR 55:331–333.

Ahmad, M.A., Puad, N.A.A., Bello, O.S. (2014) Kinetic, Equilibrium And Thermodynamic Studies of Synthetic Dye Removal Using Pomegranate Peel Activated Carbon Prepared By Microwave-Induced Koh Activation, Water Resources and Industry, http://dx.doi. org/10.1016/j.wri.2014.06.002.